Heliyon 9 (2023) e17634

Contents lists available at ScienceDirect

Heliyon

journal homepage: www.cell.com/heliyon

A general electroelastic analysis of piezoelectric shells based on levy-type solution and eigenvalue-eigenvector method

Ji Qi [a], Ran Teng [b,*], H. Elhosiny Ali [c], Mohammad Arefi [d]

[a] College of Engineering Technical, Jilin Agricultural University, Changchun, 130118, Jilin, China
[b] Northeastern Petroleum Pipeline Company, Shenyang, 110031, Liaoning, China
[c] Zagazig University, 44519, Zagazig, Egypt
[d] Faculty of Mechanical Engineering, Department of Solid Mechanics, University of Kashan, Kashan, 87317-51167, Iran

ARTICLE INFO

Keywords:
Eigenvalue-eigenvector approach
Levy type boundary conditions
Doubly curved piezoelectric shell
First order shear deformation theory

ABSTRACT

Eigenvalue-Eigenvector approach as well as Levy type solution are used for electroelastic analysis of a doubly curved shell made of piezoelectric material based on a shear deformable model and piezoelasticity relations. The electroelastic governing equations are derived using virtual work principle. The solution is proposed for a Levy type boundary conditions with two simply-supported boundary conditions and two clamped ones. After derivation of the governing equations, a solution satisfying two simply supported boundary conditions is assumed to arrive a system of ordinary differential equations. The latest governing equations are solved using Eigenvalue-Eigenvector method to satisfy clamped-clamped boundary conditions. The distribution of displacements, rotations, electric potential, strain and stress is presented along the planar coordinate. Accuracy of the proposed solution is justified through comparison with results of previous papers.

1. Introduction

Analysis of doubly curved shells because of their general shapes and geometries is very important for designer and scientists. The governing equations and the corresponding results of doubly curved shells may be reduced to arrive the results of more famous and applicable structures such as cylindrical shells and spherical shells [1–8]. Concurrently intelligent materials are applicable in electromechanical systems to sense a deflection or stress or to perform a defined work known as sensor and actuator applications. In this paper, a more general solution method is developed based on Levy technique for two simple supported and two clamped boundary conditions. A review on the recent works of doubly curved shells, piezoelectric materials and Levy type solution method is presented for justification of this new work.

Conway [9] provided a detailed analysis on the application of Levy technique for analysis of rectangular plates of variable thickness with arbitrary combination of boundary conditions. Askari Farsangi and Saidi [10] studied free vibration responses of a rectangular plate of moderately thickness sandwiched with intelligent layers based on Maxwell equations for various combination of electrical boundary conditions through a lower order shear deformable model. The numerical results have been discussed with changes of piezoelectric thickness as an important parameter. Bodaghi and Saidi [11] used a boundary layer function for buckling responses of FG plates made of FGMs. The governing equations were decomposed into to partial differential equations using the proposed function. The

* Corresponding author.
E-mail address: tengran@cnpc.com.cn (R. Teng).

https://doi.org/10.1016/j.heliyon.2023.e17634
Received 22 September 2022; Received in revised form 20 June 2023; Accepted 23 June 2023
Available online 26 June 2023

numerical results were plotted for a plate with two opposite simply supported edges with changes of geometrical and material characteristics of the plate. Thai and Choi [12] developed a refined plate theory for dynamic analyses of the functionally graded plates of different boundary conditions, where the zero surface traction at top and bottom were satisfied through this development. Using the Levy type boundary conditions, the results were compared with those lower and higher order theories as well as classical theory for verification. Amin Yekani and Fallah [13] developed a couple stress based method for small scale dependent analysis in micro sizes for Levy type bending, dynamic and stability analyses of rectangular microplates using Fourier series and state-space method and Mindlin plate theory. After verification of the results through comparison with available results of literature, effect of micro scale parameter was studied on the responses.

Saidi et al. [14] accounted stretching function in kinematic relations for bending responses of FG rectangular plate based on a higher order shear deformable model using the Levy technique. The coupled PDEs have been reduced into a lower order system using definition of novel analytical functions. Geometric nonlinear components were used for nonlinear vibration as well as control analysis of a sandwich doubly curved shell reinforced by nanocomposite sensors and actuators based on a lower order shear deformable model by Zhu et al. [15]. Impact of electric field was investigated on the responses of sandwich nanoshell with changes of nonlocal parameter. Arefi et al. [16] developed a piezoelasticity framework for dynamic analysis of a laminated sandwich cylindrical shell integrated with two piezoelectric sensor and actuator based on Hamilton's principle and considering von Karman nonlinearity and Navier's method. They found that an increase in in-homogeneous index of sensor and actuators leads to an increase in natural frequencies. Khorshidi et al. [17] developed the general formulation for dynamic response analysis of the various geometric shells integrated with piezoelectric layers reinforced with carbon nanotubes. The responses were obtained for different geometries such as cycloidal, spherical, elliptical, and toro-circular shell of revolution based on Mindlin plate theory. The governing equations were solved using GDQM for two novel electrical boundary conditions.

Movahedfar et al. [18] developed the MSGT based formulation for nonlinear vibration responses of FGP shell in micro scale and doubly curved geometry where three scale parameters were employed for a comprehensive analysis. Effect of exposed thermal and electrical loads was studied on the nonlinear vibration responses. Safaei et al. [19] summarized a comprehensive review study on the energy harvesting and its application in small scales structures and electronic devices. They expressed ability of some materials and structures in conversion of vibration energy to electrical energy. Nonlinear free vibration responses of a doubly curved micro shell made of thee phase piezoelectric material was studied based on modified strain gradient theory by Wang et al. [20]. The governing equations of motion were solved using Fourier series and Galerkin's technique to investigate impact of geometrical parameters and applied voltage on the nonlinear responses. Kiryu et al. [21] employed two variable plate theory for free vibration investigation of a plate based on Levy type method for specific boundary conditions. The responses were obtained using the frequency dependent spectral scheme. Accuracy of the proposed theory was justified through comparison with finite element results. Chen et al. [22] proposed an intelligent bistable energy harvester exposed to variable potential using a spring attached to the external magnet of a curved beam based on finite element method using COMSOL package. Magnetic dipoles method was used for nonlinear magnetic modeling. Duc et al. [23] studied effect of nonlinear strain on the vibration responses of doubly curved shell of variable material properties integrated with piezoelectric actuators in thermoelectromechanical environment and damping loading. After derivation of the governing equations of motion using third order shear deformable model, Galerkin method and 4th order Runge-Kutta were used for numerical analysis. Some applications of nano materials and structures are observed in the recent references [24–42]. Alankaya and Sinan Oktem [43] employed 3rd order theory for static analysis of cross-ply doubly curved shells. They presented some numerical results for panel subjected to point load. Tornabene and Ceruti [44] developed GDQM for static/dynamic responses multi-layered doubly curved shells/panels through a shear model where the commercial packages were used for verification. Veysi et al. [45] concurrently invstigated effect of small scale as well as nonlinear strain on the dynamic responses based on Multiple scales method. Thakur et al. [46] studied higher order shear deformation analysis of a doubly curved laminated composite shell. A new displacement function was proposed for static and free vibration analysis of the doubly curved shell. They mentioned that used method in this paper is sufficient for true determination of shear stress distribution along the thickness direction. The appropriate materials and methods for formulation of this work may be used from references [47–50]. Application of piezoelectric materials in signal processing was developed by researchers [51,52]. Some application of novel structures and energy saving in new structures were developed in references [53–57].

A relevant literature review is presented in this section with studying the related works on the doubly curved shells, piezoelectric materials and Levy-type method. The aim of this work is organization of a comprehensive methodology for electroelastic solution of a doubly curved piezoelectric shell with two simply-supported and two clamped-clamped boundary conditions. The governing equations are derived using principle of virtual work and piezoelasticity relations. After satisfying the simply-supported boundary conditions using trigonometric functions, the system of PDEs is reduced to a system of ODEs. The latest equations are solved using Eigenvalue-Eigenvector method with computations of the roots of characteristic equations and corresponding eigenvectors. The final solution will be obtained with satisfying the remained boundary condition at two clamped edges.

2. Formulation

The electroelastic formulation of a doubly curved piezoelectric shell (Fig. 1) is presented in this section based on principle of virtual work, piezoelasticity relations, a shear deformable model, Eigenvalue-Eigenvector method and Levy-type solution.

Based on the principle of virtual work, the governing equations are derived using the principle of virtual work with computation of strain energy including piezoelectric effect and external work. The variation of strain energy is defined for a doubly curved piezoelectric shell as Eq. (1) [48]:

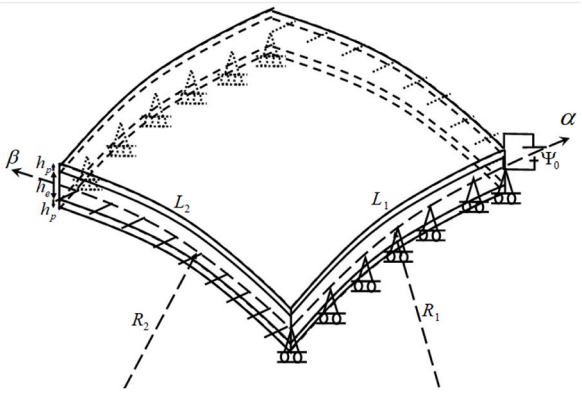

Fig. 1. The piezoelectric doubly curved shell.

$$\delta U = \int_V \{\sigma_{11}\delta\varepsilon_{11} + \sigma_{22}\delta\varepsilon_{22} + \sigma_{12}\delta\varepsilon_{12} + \sigma_{13}\delta\varepsilon_{13} + \sigma_{23}\delta\varepsilon_{23} - D_1\delta E_1 - D_2\delta E_2 - D_3\delta E_3\}dV, \tag{1}$$

In which σ_{ij} are stress components, ε_{ij} are strains, D_i and E_i are electric displacement and field, respectively. The virtual work principle (Eq. (2)) is presented as following format:

$$\delta U + \delta W = 0 \tag{2}$$

In which δW is variation of external work.

The piezoelasticity relations (Eq. (3)) are derived including stress components and electric displacements. The stress components are derived as [48]:

$$\begin{aligned} \sigma_{11} &= Q_{11}\varepsilon_{11} + Q_{12}\varepsilon_{22} - e_{11}E_3, \\ \sigma_{22} &= Q_{21}\varepsilon_{11} + Q_{22}\varepsilon_{22} - e_{23}E_3, \\ \sigma_{23} &= Q_{44}\gamma_{23} - e_{42}E_2, \\ \sigma_{13} &= Q_{55}\gamma_{13} - e_{51}E_1, \\ \sigma_{12} &= Q_{66}\gamma_{12}, \end{aligned} \tag{3}$$

where Q_{ij} are stiffness coefficients of piezoelectric material, and e_{ij} are piezoelectric coefficeints. For a piezoelectric medium, the electric displacement relations (Eq. (4)) are derived in terms of strain and electric field components as follows [48]:

$$\begin{aligned} D_1 &= e_{15}\gamma_{13} + k_{11}E_1, \\ D_{13} &= e_{24}\gamma_{23} + k_{22}E_2, \\ D_3 &= e_{31}\varepsilon_{11} + e_{32}\varepsilon_{22} + k_{33}E_3, \end{aligned} \tag{4}$$

where k_{ij} are dielectric coefficients of piezoelectric material.

To complete governing equations, it is necessary to defined kinematic relations for the doubly curved shell made of piezoelectric material. Based on a shear deformable model, the kinematic relations (Eq. (5)) are assumed as a linear function along the thickness direction as:

$$\begin{aligned} u_1 &= a_1 u + z\varphi_1, \\ v_1 &= a_2 v + z\varphi_2, \\ w_1 &= w, \end{aligned} \tag{5}$$

where u_1, v_1, w_1 are three components of displacement along the three coordinates, u, v, w are displacements of midplanes and φ_1, φ_2 are rotation components. Furthermore, $a_1 = \left(1 + \frac{z}{R_1}\right), a_2 = \left(1 + \frac{z}{R_2}\right)$, where R_1, R_2 are two principle radii of curvature. Using the shear deformable model, the strain components (Eq. (6)) are derived as follows:

$$\begin{aligned}
\varepsilon_{11} &= \frac{1}{R_1 a_1}\frac{\partial u}{\partial \alpha} + z\frac{1}{R_1 a_1}\frac{\partial \varphi_1}{\partial \alpha} + \frac{w}{R_1},\\
\varepsilon_{22} &= \frac{1}{R_2 a_2}\frac{\partial v}{\partial \beta} + z\frac{1}{R_2 a_2}\frac{\partial \varphi_2}{\partial \beta} + \frac{w}{R_2},\\
\varepsilon_{23} &= \varphi_2 + \frac{1}{R_2 a_2}\frac{\partial w}{\partial \beta} - \frac{v}{R_2},\\
\varepsilon_{13} &= \varphi_1 + \frac{1}{R_1 a_1}\frac{\partial w}{\partial \alpha} - \frac{u}{R_1},\\
\varepsilon_{12} &= \frac{1}{R_1 a_1}\frac{\partial v}{\partial \alpha} + \frac{1}{R_2 a_2}\frac{\partial u}{\partial \beta} + z\left(\frac{1}{R_1 a_1}\frac{\partial \varphi_2}{\partial \alpha} + \frac{1}{R_2 a_2}\frac{\partial \varphi_1}{\partial \beta} + \frac{1}{2}\left(\frac{1}{R_1} - \frac{1}{R_2}\right)\left(\frac{1}{R_1 a_1}\frac{\partial v}{\partial \alpha} - \frac{1}{R_2 a_2}\frac{\partial u}{\partial \beta}\right)\right),
\end{aligned} \tag{6}$$

To complete piezoelasticity relations, the electric field should be obtained so electric potential distribution $\widehat{\Psi} = \frac{2z}{h}\Psi_0 - \Psi(\alpha,\beta)cos\frac{\pi z}{h}$ satisfy Maxwell's equation (Eq. (7)) as follows [48]:

$$\begin{aligned}
E_1 &= \frac{1}{R_1 a_1}\frac{\partial \Psi}{\partial \alpha}cos\frac{\pi z}{h},\\
E_2 &= \frac{1}{R_2 a_2}\frac{\partial \Psi}{\partial \beta}cos\frac{\pi z}{h},\\
E_3 &= -\frac{2}{h}\Psi_0 - \frac{\pi}{h}\Psi\, cos\frac{\pi z}{h},
\end{aligned} \tag{7}$$

Variation of energy (Eq. (8)) is updated as:

$$\delta U = \int_A \left\{ \begin{array}{c}
\left(\frac{\partial}{\partial \alpha}\left(\frac{N_{11}}{R_1}\right) + \frac{\partial}{\partial \beta}\left(\frac{N_{12}}{R_2}\right) + \frac{N^1_{13}}{R_1} - \frac{1}{2}\left(\frac{1}{R_1} - \frac{1}{R_2}\right)\frac{\partial}{\partial \beta}\left(\frac{M_{21}}{R_2}\right)\delta u\right)\\
+\left(\frac{\partial}{\partial \alpha}\left(\frac{M_{11}}{R_1}\right) - N^1_{13} + \frac{\partial}{\partial \beta}\left(\frac{M_{21}}{R_2}\right)\right)\delta \varphi_1\\
+\left(\frac{\partial}{\partial \beta}\left(\frac{N_{22}}{R_1}\right) + \frac{\partial}{\partial \alpha}\left(\frac{N_{12}}{R_2}\right) + \frac{N^1_{23}}{R_2} + \frac{1}{2}\left(\frac{1}{R_1} - \frac{1}{R_2}\right)\frac{\partial}{\partial \alpha}\left(\frac{M_{23}}{R_1}\right)\right)\delta v\\
+\left(\frac{\partial}{\partial \beta}\left(\frac{N_{23}}{R_2}\right) + \frac{\partial}{\partial \alpha}\left(\frac{N_{13}}{R_1}\right) - \frac{N^1_{11}}{R_1} - \frac{N^1_{22}}{R_2}\right)\delta w\\
+\left(\frac{\partial}{\partial \beta}\left(\frac{M_{22}}{R_2}\right) - N^1_{23} + \frac{\partial}{\partial \alpha}\left(\frac{M_{21}}{R_2}\right)\right)\delta \varphi_2\\
+\left(\frac{\partial}{\partial \alpha}\left(\frac{\overline{D_1}}{R_1}\right) + \frac{\partial}{\partial \beta}\left(\frac{\overline{D_2}}{R_2}\right) + \overline{D_3}\right)\delta \Psi
\end{array} \right\} dA, \tag{8}$$

To complete principle of virtual work, the external work (Eq. (9)) should be computed. The external work due to uniform transverse loading is calculated as [48]:

$$\delta W = \int_A \left\{ -q\left(1 + \frac{h}{2R_1}\right)\left(1 + \frac{h}{2R_2}\right)\right\} R_1 R_2 \delta w d\alpha d\beta \tag{9}$$

Finally, the governing equations (Eq. (10)) are derived as:

$$\begin{aligned}
\delta u &: \frac{\partial}{\partial \alpha}\left(\frac{N_{11}}{R_1}\right) + \frac{\partial}{\partial \beta}\left(\frac{N_{12}}{R_2}\right) + \frac{N^1_{13}}{R_1} - \frac{1}{2}\left(\frac{1}{R_1} - \frac{1}{R_2}\right)\frac{\partial}{\partial \beta}\left(\frac{M_{21}}{R_2}\right) = 0\\
\delta \varphi_1 &: \frac{\partial}{\partial \alpha}\left(\frac{M_{11}}{R_1}\right) - N^1_{13} + \frac{\partial}{\partial \beta}\left(\frac{M_{12}}{R_2}\right) = 0\\
\delta v &: \frac{\partial}{\partial \beta}\left(\frac{N_{22}}{R_1}\right) + \frac{\partial}{\partial \alpha}\left(\frac{N_{12}}{R_2}\right) + \frac{N^1_{23}}{R_2} + \frac{1}{2}\left(\frac{1}{R_1} - \frac{1}{R_2}\right)\frac{\partial}{\partial \alpha}\left(\frac{M_{23}}{R_1}\right) = 0\\
\delta \varphi_2 &: \frac{\partial}{\partial \beta}\left(\frac{M_{22}}{R_2}\right) - N^1_{23} + \frac{\partial}{\partial \alpha}\left(\frac{M_{21}}{R_2}\right) = 0\\
\delta w &: \frac{\partial}{\partial \beta}\left(\frac{N_{23}}{R_2}\right) + \frac{\partial}{\partial \alpha}\left(\frac{N_{13}}{R_1}\right) - \frac{N^1_{11}}{R_1} - \frac{N^1_{22}}{R_2} = q\left(1 + \frac{h}{2R_1}\right)\left(1 + \frac{h}{2R_2}\right)\\
\delta \Psi &: \frac{\partial}{\partial \alpha}\left(\frac{\overline{D_1}}{R_1}\right) + \frac{\partial}{\partial \beta}\left(\frac{\overline{D_2}}{R_2}\right) + \overline{D_3} = 0
\end{aligned} \tag{10}$$

The associated boundary conditions (Eq. (11)) are derived as follows:

$$\begin{gathered}\left(\frac{N_{11}}{R_1}\right)\delta u+\left(\frac{N_{12}}{R_2}\right)\delta u-\frac{1}{2}\left(\frac{1}{R_1}-\frac{1}{R_2}\right)\frac{M_{21}}{R_2}\delta u=0\\ \left(\frac{M_{11}}{R_1}\right)\delta\varphi_1+\left(\frac{M_{12}}{R_2}\right)\delta\varphi_1=0\\ \left(\frac{N_{22}}{R_1}\right)\delta v+\left(\frac{N_{12}}{R_2}\right)\delta v+\frac{1}{2}\left(\frac{1}{R_1}-\frac{1}{R_2}\right)\left(\frac{M_{23}}{R_1}\right)\delta v=0\\ \frac{\partial}{\partial\beta}\left(\frac{M_{22}}{R_2}\right)\delta\varphi_2+\frac{\partial}{\partial\alpha}\left(\frac{M_{21}}{R_2}\right)\delta\varphi_2=0\\ \frac{\partial}{\partial\beta}\left(\frac{N_{23}}{R_2}\right)\delta w+\frac{\partial}{\partial\alpha}\left(\frac{N_{13}}{R_1}\right)\delta w=0\\ \left(\frac{\overline{D_1}}{R_1}\right)\delta\Psi+\left(\frac{\overline{D_2}}{R_2}\right)\delta\Psi+\overline{D_3}\delta\Psi=0\end{gathered}\tag{11}$$

The resultant components (Eq. (12)) are defined as follows:

$$\begin{aligned}N_{11}&=\mathscr{L}_1\frac{\partial u}{\partial\alpha}+\mathscr{L}_2 w+\mathscr{L}_3\frac{\partial\varphi_1}{\partial\alpha}+\mathscr{L}_4\frac{\partial v}{\partial\beta}+\mathscr{L}_5 w+\mathscr{L}_6\frac{\partial\varphi_2}{\partial\beta}+\mathscr{L}_7\Psi+{N_{11}}^{\Psi},N_{11}^{1}\\&=\mathscr{L}_8\frac{\partial u}{\partial\alpha}+\mathscr{L}_9 w+\mathscr{L}_{10}\frac{\partial\varphi_1}{\partial\alpha}+\mathscr{L}_{11}\frac{\partial v}{\partial\beta}+\mathscr{L}_{12} w+\mathscr{L}_{13}\frac{\partial\varphi_2}{\partial\beta}+\mathscr{L}_{14}\Psi+{N_{11}}^{1\Psi},M_{11}\\&=\mathscr{L}_{15}\frac{\partial u}{\partial\alpha}+\mathscr{L}_{16} w+\mathscr{L}_{17}\frac{\partial\varphi_1}{\partial\alpha}+\mathscr{L}_{18}\frac{\partial v}{\partial\beta}+\mathscr{L}_{19} w+\mathscr{L}_{20}\frac{\partial\varphi_2}{\partial\beta}+\mathscr{L}_{21}\Psi+{M_{11}}^{\Psi},N_{22}\\&=\mathscr{L}_4\frac{\partial u}{\partial\alpha}+\mathscr{L}_5 w+\mathscr{L}_6\frac{\partial\varphi_1}{\partial\alpha}+\mathscr{L}_{22}\frac{\partial v}{\partial\beta}+\mathscr{L}_{23} w+\mathscr{L}_{24}\frac{\partial\varphi_2}{\partial\beta}+\mathscr{L}_7\Psi+{N_{22}}^{\Psi},N_{22}^{1}\\&=\mathscr{L}_{11}\frac{\partial u}{\partial\alpha}+\mathscr{L}_{12} w+\mathscr{L}_{13}\frac{\partial\varphi_1}{\partial\alpha}+\mathscr{L}_{25}\frac{\partial v}{\partial\beta}+\mathscr{L}_{26} w+\mathscr{L}_{27}\frac{\partial\varphi_2}{\partial\beta}+\mathscr{L}_{14}\Psi+{N_{22}}^{1\Psi},M_{22}\\&=\mathscr{L}_{18}\frac{\partial u}{\partial\alpha}+\mathscr{L}_{19} w+\mathscr{L}_{20}\frac{\partial\varphi_1}{\partial\alpha}+\mathscr{L}_{28}\frac{\partial v}{\partial\beta}+\mathscr{L}_{29} w+\mathscr{L}_{30}\frac{\partial\varphi_2}{\partial\beta}+\mathscr{L}_{21}\Psi+{M_{11}}^{\Psi},N_{23}=\mathscr{L}_{31}\varphi_2+\mathscr{L}_{32}\frac{\partial w}{\partial\beta}-\mathscr{L}_{33} v-\mathscr{L}_{34}\frac{\partial\Psi}{\partial\beta},{N_{23}}^{1}\\&=\mathscr{L}_{39}\varphi_2+\mathscr{L}_{40}\frac{\partial w}{\partial\beta}-\mathscr{L}_{41} v-\mathscr{L}_{42}\frac{\partial\Psi}{\partial\beta},N_{13}=\mathscr{L}_{35}\varphi_1+\mathscr{L}_{36}\frac{\partial w}{\partial\alpha}-\mathscr{L}_{37} u-\mathscr{L}_{38}\frac{\partial\Psi}{\partial\alpha},{N_{13}}^{1}=\mathscr{L}_{43}\varphi_1+\mathscr{L}_{44}\frac{\partial w}{\partial\alpha}-\mathscr{L}_{45} u-\mathscr{L}_{46}\frac{\partial\Psi}{\partial\alpha},N_{12}\\&=\mathscr{L}_{47}\frac{\partial v}{\partial\alpha}+\mathscr{L}_{48}\frac{\partial u}{\partial\beta}+\mathscr{L}_{49}\frac{\partial\varphi_2}{\partial\alpha}+\mathscr{L}_{50}\frac{\partial\varphi_1}{\partial\beta}+\mathscr{L}_{51}\frac{\partial v}{\partial\alpha}-\mathscr{L}_{52}\frac{\partial u}{\partial\beta},N_{21}=\mathscr{L}_{53}\frac{\partial v}{\partial\alpha}+\mathscr{L}_{54}\frac{\partial u}{\partial\beta}+\mathscr{L}_{55}\frac{\partial\varphi_2}{\partial\alpha}+\mathscr{L}_{56}\frac{\partial\varphi_1}{\partial\beta}+\mathscr{L}_{57}\frac{\partial v}{\partial\alpha}-\mathscr{L}_{58}\frac{\partial u}{\partial\beta},M_{12}\\&=\mathscr{L}_{59}\frac{\partial v}{\partial\alpha}+\mathscr{L}_{60}\frac{\partial u}{\partial\beta}+\mathscr{L}_{61}\frac{\partial\varphi_2}{\partial\alpha}+\mathscr{L}_{62}\frac{\partial\varphi_1}{\partial\beta}+\mathscr{L}_{63}\frac{\partial v}{\partial\alpha}-\mathscr{L}_{64}\frac{\partial u}{\partial\beta},M_{21}=\mathscr{L}_{65}\frac{\partial v}{\partial\alpha}+\mathscr{L}_{66}\frac{\partial u}{\partial\beta}+\mathscr{L}_{67}\frac{\partial\varphi_2}{\partial\alpha}+\mathscr{L}_{68}\frac{\partial\varphi_1}{\partial\beta}+\mathscr{L}_{69}\frac{\partial v}{\partial\alpha}-\mathscr{L}_{70}\frac{\partial u}{\partial\beta},\overline{D}_1\\&=\mathscr{L}_{71}\varphi_1+\mathscr{L}_{72}\frac{\partial w}{\partial\alpha}-\mathscr{L}_{73} u-\mathscr{L}_{74}\frac{\partial\Psi}{\partial\alpha},\overline{D}_2=\mathscr{L}_{75}\varphi_2+\mathscr{L}_{76}\frac{\partial w}{\partial\beta}-\mathscr{L}_{77} v-\mathscr{L}_{78}\frac{\partial\Psi}{\partial\beta},D_3\\&=\mathscr{L}_{79}\frac{\partial u}{\partial\alpha}+\mathscr{L}_{80} w+\mathscr{L}_{81}\frac{\partial\varphi_1}{\partial\alpha}+\mathscr{L}_{82}\frac{\partial v}{\partial\beta}+\mathscr{L}_{83} w+\mathscr{L}_{84}\frac{\partial\varphi_2}{\partial\beta}+\mathscr{L}_{85}\Psi+{D_z}^{\Psi}\end{aligned}\tag{12}$$

Finally, the governing equations (Eq. 13a-f) are presented as:

$$\delta u:L_{11}u+L_{12}\varphi_1+L_{13}v+L_{14}\varphi_2+L_{15}w+L_{16}\Psi=0\tag{13a}$$

$$\delta\varphi_1:L_{21}u+L_{22}\varphi_1+L_{23}v+L_{24}\varphi_2+L_{25}w+L_{26}\Psi=0\tag{13b}$$

$$\delta v:L_{31}u+L_{32}\varphi_1+L_{33}v+L_{34}\varphi_2+L_{35}w+L_{36}\Psi=0\tag{13c}$$

$$\delta\varphi_2:L_{41}u+L_{42}\varphi_1+L_{43}v+L_{44}\varphi_2+L_{45}w+L_{46}\Psi=0\tag{13d}$$

$$\delta w:L_{51}u+L_{52}\varphi_1+L_{53}v+L_{54}\varphi_2+L_{55}w+L_{56}\Psi=+\frac{{N_{11}}^{1\Psi}}{R_1}+\frac{{N_{22}}^{1\Psi}}{R_2}+q\left[1+\frac{h}{2R_1}\right]\left[1+\frac{h}{2R_2}\right]\tag{13e}$$

$$\delta\Psi:L_{61}u+L_{62}\varphi_1+L_{63}v+L_{64}\varphi_2+L_{65}w+L_{66}\Psi=-{D_z}^{\Psi}\tag{13f}$$

In which the operators L_{ij} (Eq. 14a-f) are defined as follows:

$$\begin{aligned}
&u: L_{11}=\frac{\mathscr{L}_1}{R_1}\frac{\partial^2(..)}{\partial\alpha^2}+\left(\frac{\chi[\mathscr{L}_{70}-\mathscr{L}_{66}]+\mathscr{L}_{54}-\mathscr{L}_{58}}{R_2}\right)\frac{\partial^2(..)}{\partial\beta^2}-\frac{\mathscr{L}_{45}}{R_1}, L_{12}=\frac{\mathscr{L}_3}{R_1}\frac{\partial^2(..)}{\partial\alpha^2}+\left(\frac{\mathscr{L}_{56}-\chi\mathscr{L}_{68}}{R_2}\right)\frac{\partial^2(..)}{\partial\beta^2}+\frac{\mathscr{L}_{43}}{R_1},\\
&L_{13}=\frac{\mathscr{L}_4}{R_1}\frac{\partial^2(..)}{\partial\alpha\partial\beta}+\left(\frac{\mathscr{L}_{57}+\mathscr{L}_{53}-\chi[\mathscr{L}_{65}+\mathscr{L}_{69}]}{R_2}\right)\frac{\partial^2(..)}{\partial\alpha\partial\beta}, L_{14}=\left(\frac{\mathscr{L}_6}{R_1}+\frac{\mathscr{L}_{55}-\chi\mathscr{L}_{67}}{R_2}\right)\frac{\partial^2(..)}{\partial\alpha\partial\beta},\\
&L_{15}=\left(\frac{\mathscr{L}_5+\mathscr{L}_2+\mathscr{L}_{44}}{R_1}\right)\frac{\partial(..)}{\partial\alpha}, L_{16}=\left(\frac{\mathscr{L}_7-\mathscr{L}_{46}}{R_1}\right)\frac{\partial(..)}{\partial\alpha}
\end{aligned}\tag{14a}$$

$$\begin{aligned}
&\delta\varphi_1: L_{21}=\frac{\mathscr{L}_{15}}{R_1}\frac{\partial^2(..)}{\partial\alpha^2}+\frac{(\mathscr{L}_{66}-\mathscr{L}_{70})}{R_2}\frac{\partial^2(..)}{\partial\beta^2}+\mathscr{L}_{45}, L_{22}=\frac{\mathscr{L}_{17}}{R_1}\frac{\partial^2(..)}{\partial\alpha^2}+\frac{\mathscr{L}_{68}}{R_2}\frac{\partial^2(..)}{\partial\beta^2}-\mathscr{L}_{43}, L_{23}=\left(\frac{\mathscr{L}_{65}+\mathscr{L}_{69}}{R_2}+\frac{\mathscr{L}_{18}}{R_1}\right)\frac{\partial^2(..)}{\partial\alpha\partial\beta},\\
&L_{24}=\left(\frac{\mathscr{L}_{20}}{R_1}+\frac{\mathscr{L}_{67}}{R_2}\right)\frac{\partial(..)}{\partial\alpha\partial\beta}\varphi_2, L_{25}=\left(\frac{\mathscr{L}_{19}+\mathscr{L}_{16}}{R_1}-\mathscr{L}_{44}\right)\frac{\partial(..)}{\partial\alpha}, L_{26}=\left(\frac{\mathscr{L}_{21}}{R_1}+\mathscr{L}_{46}\right)\frac{\partial(..)}{\partial\alpha}
\end{aligned}\tag{14b}$$

$$\begin{aligned}
&\delta v: L_{31}=\left(\frac{\mathscr{L}_4}{R_2}+\frac{\chi[\mathscr{L}_{60}-\mathscr{L}_{64}]+\mathscr{L}_{48}-\mathscr{L}_{52}}{R_1}\right)\frac{\partial^2(..)}{\partial\alpha\partial\beta}, L_{32}=\left(\frac{\mathscr{L}_{50}+\chi\mathscr{L}_{62}}{R_1}+\frac{\mathscr{L}_6}{R_2}\right)\frac{\partial^2(..)}{\partial\alpha\partial\beta},\\
&L_{33}=\left(\frac{\mathscr{L}_{47}+\mathscr{L}_{51}+\chi[\mathscr{L}_{59}+\mathscr{L}_{63}]}{R_1}\right)\frac{\partial^2(..)}{\partial\alpha^2}+\frac{\mathscr{L}_{22}}{R_2}\frac{\partial^2(..)}{\partial\beta^2}-\frac{\mathscr{L}_{41}}{R_2}, L_{34}=\left(\frac{\mathscr{L}_{49}+\chi\mathscr{L}_{61}}{R_1}\right)\frac{\partial^2(..)}{\partial\alpha^2}+\frac{\mathscr{L}_{24}}{R_2}\frac{\partial^2(..)}{\partial\beta^2}+\frac{\mathscr{L}_{39}}{R_2},\\
&L_{35}=\left(\frac{\mathscr{L}_{40}+\mathscr{L}_5+\mathscr{L}_{23}}{R_2}\right)\frac{\partial(..)}{\partial\beta}, L_{36}=\left(\frac{\mathscr{L}_7-\mathscr{L}_{42}}{R_2}\right)\frac{\partial(..)}{\partial\beta}
\end{aligned}\tag{14c}$$

$$\begin{aligned}
&\delta\varphi_2: L_{41}=\left(\frac{\mathscr{L}_{18}}{R_2}+\frac{\mathscr{L}_{60}-\mathscr{L}_{64}}{R_1}\right)\frac{\partial^2(..)}{\partial\alpha\partial\beta}, L_{42}=\left(\frac{\mathscr{L}_{62}}{R_1}+\frac{\mathscr{L}_{20}}{R_2}\right)\frac{\partial^2(..)}{\partial\alpha\partial\beta}, L_{43}=\left(\frac{\mathscr{L}_{59}+\mathscr{L}_{63}}{R_1}\right)\frac{\partial^2(..)}{\partial\alpha^2}+\frac{\mathscr{L}_{28}}{R_2}\frac{\partial^2(..)}{\partial\beta^2}+\mathscr{L}_{41},\\
&L_{44}=\left(\frac{\mathscr{L}_{30}}{R_2}+\frac{\mathscr{L}_{61}}{R_1}\right)\frac{\partial^2(..)}{\partial\alpha^2}-\mathscr{L}_{39}\varphi_2, L_{45}=\left(\frac{\mathscr{L}_{29}+\mathscr{L}_{19}}{R_2}-\mathscr{L}_{40}\right)\frac{\partial(..)}{\partial\beta}, L_{46}=\left(\frac{\mathscr{L}_{21}}{R_2}+\mathscr{L}_{42}\right)\frac{\partial(..)}{\partial\beta}
\end{aligned}\tag{14d}$$

$$\begin{aligned}
&\delta w: L_{51}=\left(-\frac{\mathscr{L}_{11}}{R_2}-\frac{\mathscr{L}_8+\mathscr{L}_{37}}{R_1}\right)\frac{\partial(..)}{\partial\alpha}, L_{52}=\left(\frac{\mathscr{L}_{35}-\mathscr{L}_{10}}{R_1}-\frac{\mathscr{L}_{13}}{R_2}\right)\frac{\partial(..)}{\partial\alpha}, L_{53}=\left(-\frac{\mathscr{L}_{33}+\mathscr{L}_{25}}{R_2}-\frac{\mathscr{L}_{11}}{R_1}\right)\frac{\partial(..)}{\partial\beta},\\
&L_{54}=\left(-\frac{\mathscr{L}_{27}}{R_2}-\frac{\mathscr{L}_{13}}{R_1}-\frac{\mathscr{L}_{31}}{R_2}\right)\frac{\partial(..)}{\partial\beta}, L_{55}=\left(-\frac{\mathscr{L}_9+\mathscr{L}_{12}}{R_1}-\frac{\mathscr{L}_{12}+\mathscr{L}_{26}}{R_2}\right)+\frac{\mathscr{L}_{36}}{R_1}\frac{\partial^2(..)}{\partial\alpha^2},\\
&L_{56}=\left(\frac{\mathscr{L}_{32}-\mathscr{L}_{34}}{R_2}\right)\frac{\partial^2(..)}{\partial\beta^2}-\frac{\mathscr{L}_{38}}{R_1}\frac{\partial^2(..)}{\partial\alpha^2}+\left(-\frac{\mathscr{L}_{14}}{R_2}-\frac{\mathscr{L}_{14}}{R_1}\right), F_5=+\frac{N_{11}{}^{1\Psi}}{R_1}+\frac{N_{22}{}^{1\Psi}}{R_2}+q\left[1+\frac{h}{2R_1}\right]\left[1+\frac{h}{2R_2}\right]
\end{aligned}\tag{14e}$$

$$\begin{aligned}
&\delta\Psi: L_{61}=\left(-\frac{\mathscr{L}_{73}}{R_1}+\mathscr{L}_{79}\right)\frac{\partial(..)}{\partial\alpha}, L_{62}=\left(\frac{\mathscr{L}_{71}}{R_1}+\mathscr{L}_{81}\right)\frac{\partial(..)}{\partial\alpha}, L_{63}=\left(\mathscr{L}_{82}-\frac{\mathscr{L}_{77}}{R_2}\right)\frac{\partial(..)}{\partial\beta}, L_{64}=\left(\frac{\mathscr{L}_{75}}{R_2}+\mathscr{L}_{84}\right)\frac{\partial(..)}{\partial\beta},\\
&L_{65}=\frac{\mathscr{L}_{72}}{R_1}\frac{\partial^2(..)}{\partial\alpha^2}+\frac{\mathscr{L}_{76}}{R_2}\frac{\partial^2(..)}{\partial\beta^2}+(\mathscr{L}_{80}+\mathscr{L}_{83}), L_{66}=-\frac{\mathscr{L}_{78}}{R_2}\frac{\partial^2(..)}{\partial\beta^2}-\frac{\mathscr{L}_{74}}{R_1}\frac{\partial^2(..)}{\partial\alpha^2}+\mathscr{L}_{85}, F_6=-D_z{}^{\Psi}
\end{aligned}\tag{14f}$$

3. Solution

In this section, the solution methodology is presented for two opposite simply supported and two opposite clamped-clamped boundary conditions. For this purpose, the Levy type method is used.

The required boundary conditions (Eq. (15)) are assumed as follows:

$$\begin{aligned}
&\beta=0,\frac{L_2}{R_2}: u=\varphi_1=w=\Psi=0\\
&\alpha=0,\frac{L_1}{R_2}: u=\varphi_1=v=\varphi_2=w=\Psi=0
\end{aligned}\tag{15}$$

To satisfy two opposite simply-supported boundary conditions along β direction, the solution (Eq. (16)) is assumed as [49,50]:

$$\begin{Bmatrix} u\\ \varphi_1\\ v\\ \varphi_2\\ w\\ \Psi \end{Bmatrix}=\begin{Bmatrix} U(\alpha)\sin\mu_n\beta\\ \Phi_1(\alpha)\sin\mu_n\beta\\ V(\alpha)\cos\mu_n\beta\\ \Phi_2(\alpha)\cos\mu_n\beta\\ W(\alpha)\sin\mu_n\beta\\ \Psi(\alpha)\sin\mu_n\beta \end{Bmatrix}\tag{16}$$

in which $\mu_n = n\pi R_2/L_2$. The system of ordinary differential equations can be solved analytically for any boundary conditions using the Eigenvalue-Eigenvector method. The homogeneous solution (Eq. (17)) based on Eigenvalue-Eigenvector method is assumed as [49]:

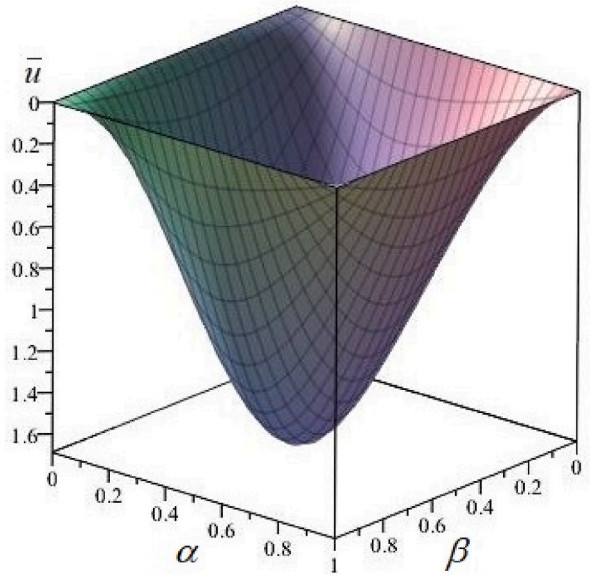

Fig. 2. Variation of in-plane displacement $\bar{u}$ along the planar direction (α, β).

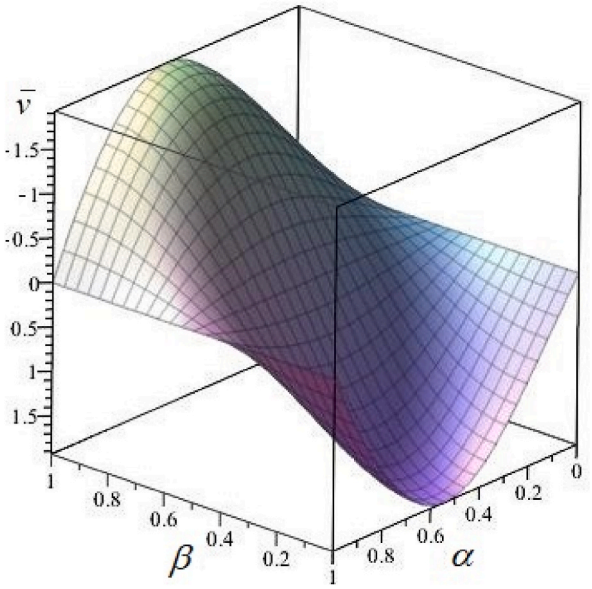

Fig. 3. Variation of in-plane displacement $\bar{v}$ along the planar direction (α, β).

$$\begin{Bmatrix} \mathrm{U}(\alpha) \\ \Phi_1(\alpha) \\ \mathrm{V}(\alpha) \\ \Phi_2(\alpha) \\ \mathrm{W}(\alpha) \\ \Psi(\alpha) \end{Bmatrix} = \sum_i \begin{Bmatrix} \widetilde{\mathrm{U}}_i e^{m_i x} \\ \widetilde{\Phi_{1i}} e^{m_i x} \\ \widetilde{\mathrm{V}}_i e^{m_i x} \\ \widetilde{\Phi_{2i}} e^{m_i x} \\ \widetilde{\mathrm{W}}_i e^{m_i x} \\ \widetilde{\Psi}_i e^{m_i x} \end{Bmatrix} \tag{17}$$

in which m_i are eigenvalues, and i is order of characteristic equations. The magnitude of eigenvalues is obtained using solution of the characteristic equation.

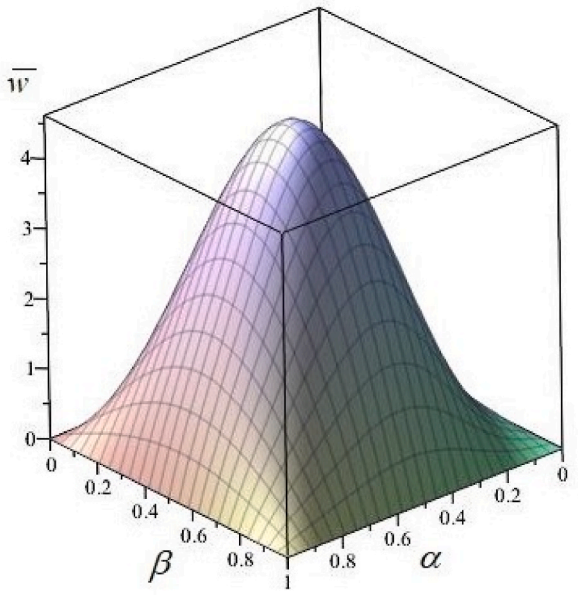

Fig. 4. Variation of transverse deflection $\overline{w}$ along the planar direction (α, β).

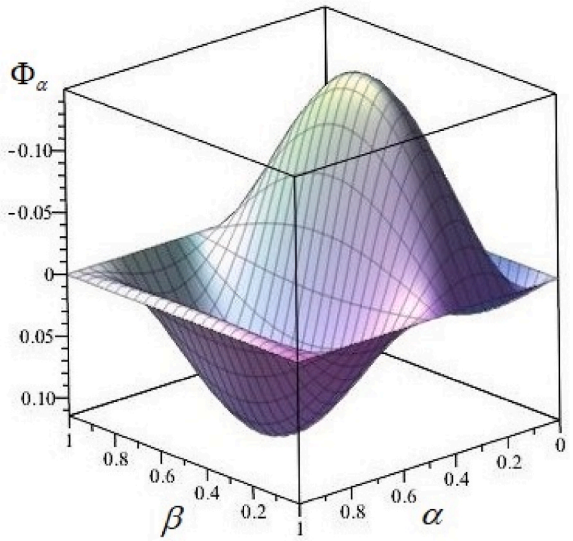

Fig. 5. Variation of rotation component φ_α along the planar direction (α, β).

4. Numerical results and discussion

After explanation of the solution procedure, the numerical results are presented in this section. The numerical results are computed for the following material properties:

$Q_{11} = 138.499$ GPa.$Q_{22} = 138.499$ GPa.$Q_{33} = 114.745$ GPa

$Q_{12} = 77.371$ GPa. $Q_{13} = 73.643$ GPa, $Q_{23} = 73.643$ GPa

$Q_{44} = 25.6$ GPa.$Q_{55} = 25.6$ GPa.$Q_{66} = 30.6$ GPa

$e_{13} = e_{31} = -5.2\,C/m^2$. $e_{23} = e_{32} = -5.2\,C/m^2$. $e_{33} = 15.8\,C/m^2$.$e_{15} = 12.72\,C/m^2$.$e_{24} = 12.72\,C/m^2$

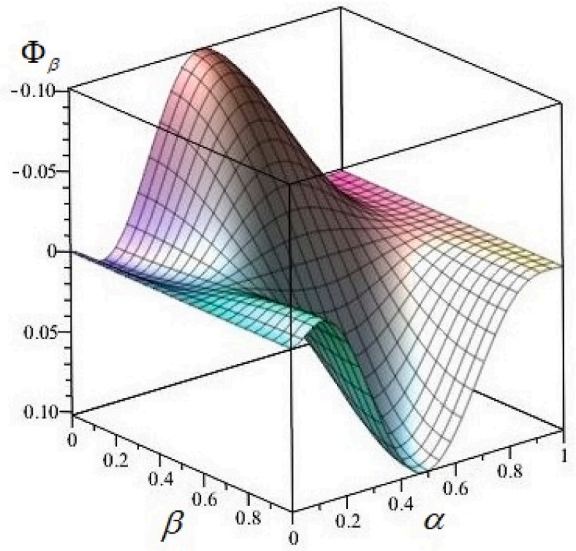

Fig. 6. Variation of rotation component φ_β along the planar direction (α, β).

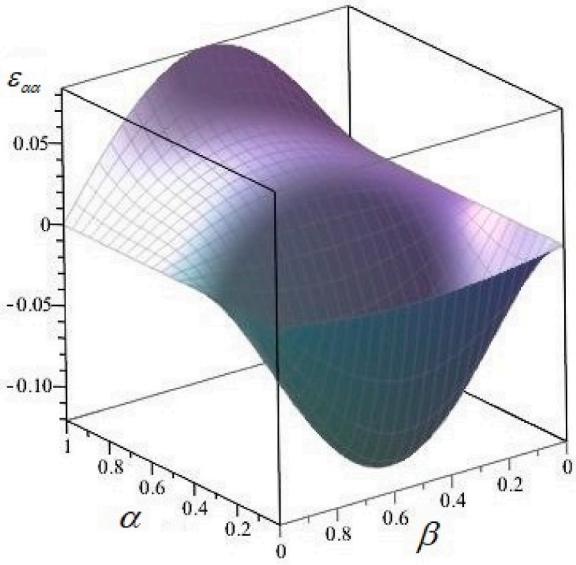

Fig. 7. Variation of in-plane normal strain $\varepsilon_{\alpha\alpha}$ along the planar direction (α, β).

$$k_{11} = 1.306 \times 10^{-8} \mathrm{F/_m}.k_{22} = 1.306 \times 10^{-8} \mathrm{F/_m}.k_{33} = 1.151 \times 10^{-8} \mathrm{F/_m}$$

in which the material properties are belong to PZT-4. Before presentation of the full numerical results, a comparative study is needed for verification and validation of the solution procedure.

Figs. 2 and 3 show changes of two in-plane displacements $\overline{u,v}$ along the planar direction (α, β). The results are obtained for two simply supported and two clamped boundary conditions. It is observed that maximum displacement $\overline{u}$ is occurred at middle of the doubly curved shell while the maximum is occurred at middle of both ends $\beta = 0, 1$.

Fig. 4 shows variation of transverse deflection $\overline{w}$ along the planar direction (α, β). It is deduced that the maximum transverse deflection is occurred at middle of the shell. It is concluded that the transverse deflection is a dominant component between all deformation components with significant value.

Figs. 5 and 6 show variation of two rotation components along the planar coordinate. It is observed that the maximum first rotation component is occurred at the location between mid-length and two ends of the shell while the second rotation component is occurred at middle of the shell edges.

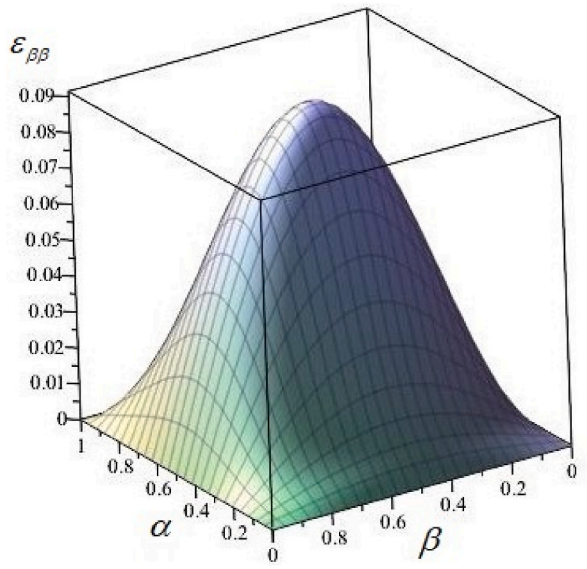

Fig. 8. Variation of in-plane normal strain $\varepsilon_{\beta\beta}$ along the planar direction (α, β).

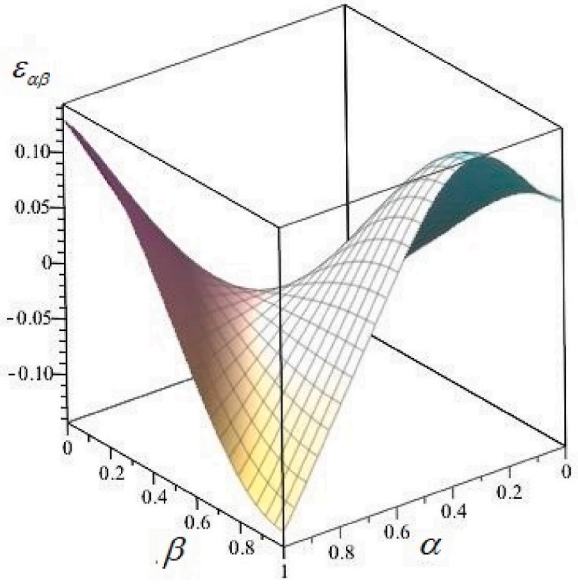

Fig. 9. Variation of in-plane shear strain $\gamma_{\alpha\beta}$ along the planar direction (α, β).

Figs. 7 and 8 show variation of in-plane normal strains $\varepsilon_{\alpha\alpha}, \varepsilon_{\beta\beta}$ along the planar direction (α, β). It is observed that the maximum normal strain $\varepsilon_{\alpha\alpha}$ is occurred at near the clamed edges because of abrupt changes of the shape of the shell. Furthermore, the maximum normal strain $\varepsilon_{\beta\beta}$ is occurred at center of the shell.

Shown in Fig. 9 is variation of in-plane shear strain $\gamma_{\alpha\beta}$ along the planar direction (α, β). It is observed that the maximum in-plane shear strain $\gamma_{\alpha\beta}$ is occurred at four corners of the shell.

Shown in Figs. 10 and 11 are depiction of the out of plane shear strain components $\gamma_{\alpha z}, \gamma_{\beta z}$ along the x and y directions. It is concluded that the maximum shearing strain $\gamma_{\alpha z}$ is occurred at middle of clamped edges. One can conclude that occurring the significant value of out of plane shear strain is because of presence of clamped edge and abrupt changes of the shell. Furthermore the maximum shearing strain $\gamma_{\beta z}$ is occurred at middle of simply supported edges.

Shown in Figs. 12 and 13 are variation of in-plane normal stresses $\overline{\sigma_{\alpha\alpha}}$, $\overline{\sigma_{\beta\beta}}$ along the planar direction (α, β). It is observed that the maximum normal stresses $\overline{\sigma_{\alpha\alpha}}$, $\overline{\sigma_{\beta\beta}}$ are occurred at nearing the clamped edges. It is concluded that the clamped boundary conditions lead to significant and abrupt changes of deformation and strain and consequently significant stress.

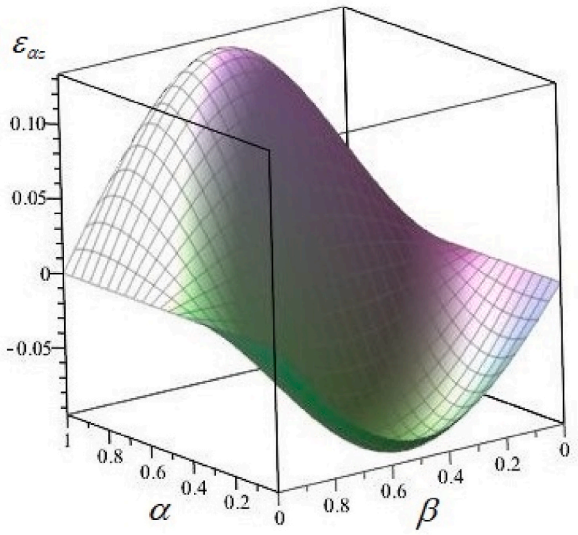

Fig. 10. Variation of out of plane shear strain $\gamma_{\alpha z}$ along the planar direction (α, β).

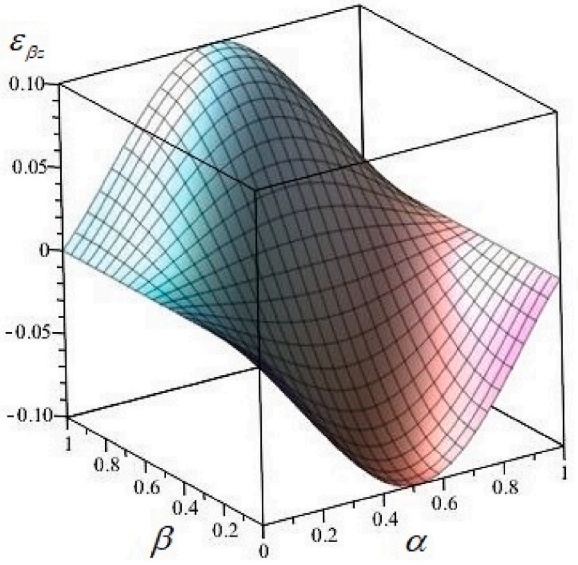

Fig. 11. Variation of out of plane shear strain $\gamma_{\beta z}$ along the planar direction (α, β).

5. Conclusion

Electroelastic analysis of a doubly curved shell made of piezoelectric material was studied in this paper based on a shear deformable kinematic model, piezoelasticity relations and Levy-type method. The governing equations were derived based on virtual work principle with computation of strain energy and external work. The Levy-type boundary condition is considered for the doubly curved shell with two simply supported and two clamped-clamped boundary conditions. Eigenvalue-Eigenvector method is used for the solution of assumed boundary conditions. The numerical results including displacements, strain and stress components along the planar coordinates are presented. The main results of this work are expressed as:

Investigating changes of in-plane displacements indicates that maximum displacement $\bar{u}$ is occurred at middle of the doubly curved shell while the maximum $\bar{v}$ is occurred at middle of both ends $\beta = 0, 1$. Furthermore, it is observed that the maximum first rotation component is occurred at the location between mid-length and two ends of the shell.

Investigating changes of out of plane shear strain components $\gamma_{\alpha z}, \gamma_{\beta z}$ indicates that the maximum shearing strain $\gamma_{\alpha z}$ is occurred at middle of clamped edges. Furthermore the maximum shearing strain $\gamma_{\beta z}$ is occurred at middle of simply supported edges.

Changes of in-plane normal stresses indicates that the maximum normal stresses and strains $\overline{\sigma_{\alpha\alpha}}$, $\varepsilon_{\alpha\alpha}$, $\overline{\sigma_{\beta\beta}}$, $\varepsilon_{\beta\beta}$ are occurred at nearing

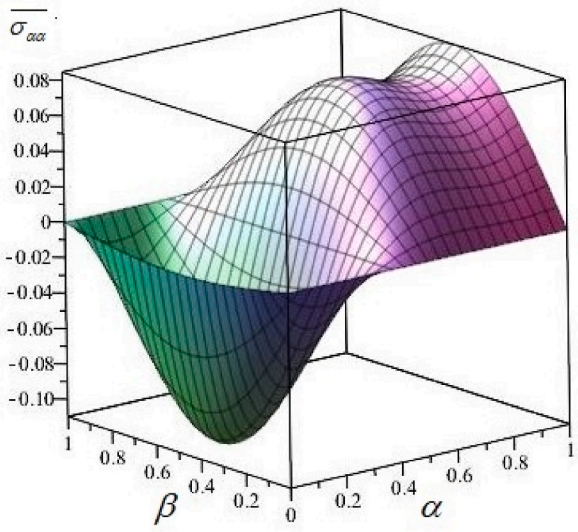

Fig. 12. Variation of in-plane normal stress $\overline{\sigma_{\alpha\alpha}}$ along the planar direction (α, β).

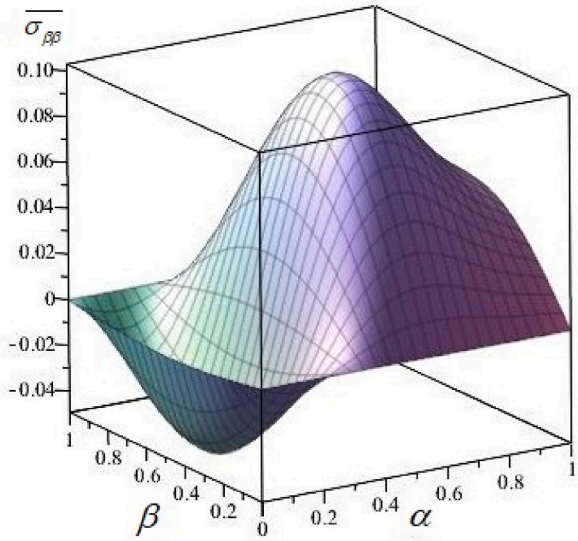

Fig. 13. Variation of in-plane normal stress $\sigma_{\beta\beta}$ along the planar direction (α, β).

the clamped edges. Furthermore, the maximum in-plane shear stress σ_{xy} is occurred at both corners of clamed edges. The maximum shear stresses are occurred at middle of simply supported edges. Furthermore, the maximum in-plane shear strain $\gamma_{\alpha\beta}$ is occurred at four corners of the shell.

Funding

National Natural Science Foundation of China Science and Technology Development Program Foundation of Jilin Province Scientific Reseaīrch Foundation of Jilin Provincial Ecological Environment Department The Capital Construction Program Foundation within the Budget of Jilin Province Scientific Research Foundation of Jilin Provincial Education Department.

Author contribution statement

Ji Qi, H. Elhosiny Ali: Analyzed and interpreted the data; Wrote the paper.
Ran Teng: Analyzed and interpreted the data; Contributed analysis tools or data; Wrote the paper.
Mohammad Arefi: Conceived and designed the analysis; Analyzed and interpreted the data; Contributed analysis tools or data;

Wrote the paper.

Data availability statement

No data was used for the research described in the article.

Declaration of competing interest

The authors declare that they have no known competing financial interests or personal relationships that could have appeared to influence the work reported in this paper

References

[1] X. Meng, R.O. Suzuki, Simulation analysis of tilted polyhedron-shaped thermoelectric elements, J. Electron. Mater. 44 (6) (2015) 1469–1476, https://doi.org/10.1007/s11664-014-3418-5.
[2] B. Zheng, Y. Liu, M. Yu, Y. Jin, Q. Zhang, Q. Chen, Flow control performance evaluation of tri-electrode sliding discharge plasma actuator, Chin. Phys. B (2022), https://doi.org/10.1088/1674-1056/acae76.
[3] S. Lu, Z. Yin, S. Liao, B. Yang, S. Liu, M. Liu, W. Zheng, An asymmetric encoder–decoder model for Zn-ion battery lifetime prediction, Energy Rep. 8 (2022) 33–50, https://doi.org/10.1016/j.egyr.2022.09.211.
[4] X. Xiao, Q. Zhang, J. Zheng, Z. Li, Analytical model for the nonlinear buckling responses of the confined polyhedral FGP-GPLs lining subjected to crown point loading, Eng. Struct. 282 (2023), 115780, https://doi.org/10.1016/j.engstruct.2023.115780.
[5] T. Gao, Y. Zhang, C. Li, Y. Wang, Y. Chen, Q. An, S. Zhang, H.N. Li, H. Cao, H.M. Ali, Z. Zhou, S. Sharma, Fiber-reinforced composites in milling and grinding. machining bottlenecks and advanced strategies, Front. Mech. Eng. 17 (2) (2022) 24.
[6] X. Cui, C. Li, Y. Zhang, Z. Said, S. Debnath, S. Sharma, H.M. Ali, M. Yang, T. Gao, R. Li, Grindability of titanium alloy using cryogenic nanolubricant minimum quantity lubrication, J. Manuf. Process. 80 (2022) 273–286.
[7] X. Wang, C. Li, Y. Zhang, H.M. Ali, S. Sharma, R. Li, M. Yang, Z. Said, X. Liu, Tribology of enhanced turning using biolubricants, A comparative assessment, Trib. Int. (2022), 107766.
[8] W. Xu, C. Li, Y. Zhang, H.M. Ali, S. Sharma, R. Li, M. Yang, T. Gao, M. Liu, X. Wang, Z. Said, X. Liu, Z. Zou, Electrostatic atomization minimum quantity lubrication machining. from mechanism to application, Int. J. Extrem. Manuf. 4 (2022), 042003.
[9] H.D. Conway, A levy-type solution for a rectangular plate of variable thickness, J. Appl. Mech. 25 (2) (1958) 297–298.
[10] M.A. Askari Farsangi, A.R. Saidi, Levy type solution for free vibration analysis of functionally graded rectangular plates with piezoelectric layers, Smart Mater. Struct. 21 (9) (2012), 094017.
[11] M. Bodaghi, A.R. Saidi, Levy-type solution for buckling analysis of thick functionally graded rectangular plates based on the higher-order shear deformation plate theory, Appl. Math. Model. 34 (11) (2010) 3659–3673.
[12] H.-T. Thai, D.-H. Choi, Levy solution for free vibration analysis of functionally graded plates based on a refined plate theory, KSCE J. Civ. Eng. 18 (2014) 1813–1824.
[13] S.M. Amin Yekani, F. Fallah, A Levy solution for bending, buckling, and vibration of Mindlin micro plates with a modified couple stress theory, SN Appl. Sci. 2 (2020) 2169.
[14] A.R. Saidi, M. Bodaghi, S.R. Atashipour, Levy-type solution for bending-stretching of thick functionally graded rectangular plates based on third-order shear deformation theory, Mech. Adv. Mater. Struct. 19 (8) (2012) 577–589.
[15] C. Zhu, X. Fang, J. Liu, G. Nie, C. Zhang, An analytical solution for nonlinear vibration control of sandwich shallow doubly-curved nanoshells with functionally graded piezoelectric nanocomposite sensors and actuators, Mech. Based, Design. Struct. Mach. 50 (7) (2022) 2508–2534.
[16] M. Arefi, R. Karroubi, M. Irani-Rahaghi, Free vibration analysis of functionally graded laminated sandwich cylindrical shells integrated with piezoelectric layer, Appl. Math. Mech. 37 (2016) 821–834.
[17] S. Khorshidi, S. Saber-Samandari, M. Salehi, Free vibration response of functionally graded carbon nanotubes double curved shell and panel with piezoelectric layers in a thermal environment, Sci. Iranica., Trans. Mech. Eng. (B) 27 (5) (2020) 2391–2408.
[18] V. Movahedfar, M.M. Kheirikhah, Y. Mohammadi, F. Ebrahimi, Modified strain gradient theory for nonlinear vibration analysis of functionally graded piezoelectric doubly curved microshells, Proc. Inst. Mech. Eng., .C. J. Mech. Eng. Sci. 236 (8) (2022) 4219–4231.
[19] M. Safaei, H.A. Sodano, S.R. Anton, A review of energy harvesting using piezoelectric materials. state-of-the-art a decade later, Smart Mater. Struct. 28 (2019), 113001.
[20] D. Wang, Y. Xing, S. Zhang, Nonlinear electromechanical dynamics of piezoelectric doubly-curved microsystem using modified strain gradient theory, Adv. Nano. Res. 11 (4) (2021) 381–392.
[21] S. Kiryu, S.W. Alisjahbana, I. Alisjahbana, M. Nagao, B.S. Gan, Free vibration of a Levy-type solution for plates based on two-variable refined plate theory by using SEM, J. Vibroeng. 21 (3) (2019) 726–735, https://doi.org/10.21595/jve.2018.20431.
[22] X. Chen, X. Zhang, L. Chen, Y. Guo, F. Zhu, A curve-shaped beam bistable piezoelectric energy harvester with variable potential well. Modeling and numerical simulation, Micromachines 12 (8) (2021) 995.
[23] N.D. Duc, T.Q. Quan, V.D. Luat, Nonlinear dynamic analysis and vibration of shear deformable piezoelectric FGM double curved shallow shells under damping-thermo-electro-mechanical loads, Compos. Struct. 125 (2015) 29–40.
[24] F. Song, Y. Liu, W. Jin, J. Tan, W, Data-driven feedforward learning with force ripple compensation for wafer stages. A variable-gain robust approach, IEEE Transact. Neural Networks Learn. Syst. 33 (4) (2022) 1594–1608, https://doi.org/10.1109/TNNLS.2020.3042975.
[25] X. Meng, R.O. Suzuki, Performance analysis of thermoelectric modules using polyhedron elements, Mater. Trans. 56 (7) (2015) 1092–1095, https://doi.org/10.2320/matertrans. E-M2015808.
[26] W. Dang, S. Liao, B. Yang, Z. Yin, M. Liu, L. Yin, W. Zheng, An encoder-decoder fusion battery life prediction method based on Gaussian process regression and improvement, J. Energy Storage 59 (2023), 106469, https://doi.org/10.1016/j.est.2022.106469.
[27] Z. Zhang, Q. Yang, Z. Yu, H. Wang, T. Zhang, Influence of Y2O3 addition on the microstructure of TiC reinforced Ti-based composite coating prepared by laser cladding, Mater. Char. (2022) 189, https://doi.org/10.1016/j.matchar.2022.111962.
[28] L. Guo, C. Ye, Y. Ding, P. Wang, Allocation of centrally switched fault current limiters enabled by 5G in transmission system, IEEE Trans. Power Deliv. 36 (5) (2021) 3231–3241, https://doi.org/10.1109/TPWRD.2020.3037193.
[29] H. Lu, Y. Zhu, M. Yin, G. Yin, L. Xie, Multimodal fusion convolutional neural network with cross-attention mechanism for internal defect detection of magnetic tile, IEEE Access 10 (2022) 60876–60886, https://doi.org/10.1109/ACCESS.2022.3180725.
[30] H. Wang, B. Wang, P. Luo, F. Ma, Y. Zhou, M.A. Mohamed, State evaluation based on feature identification of measurement data. For resilient power system, CSEE. J. Power. Energy. Syst. 8 (4) (2022) 983–992, https://doi.org/10.17775/CSEEJPES.2021.01270.
[31] J. Gao, H. Sun, J. Han, Q. Sun, T. Zhong, Research on recognition method of electrical components based on FEYOLOv4-tiny, J. Electr. Eng. Technol. (2022), https://doi.org/10.1007/s42835-022-01124-0.
[32] M. Yang, C. Li, Y. Zhang, D. Jia, X. Zhang, Y. Hou, R. Li, J. Wang, Maximum undeformed equivalent chip thickness for ductile-brittle transition of zirconia ceramics under different lubrication conditions, Int. J. Mach. Tool Manufact. 122 (2017) 55–65.

[33] B. Li, C. Li, Y. Zhang, Y. Wang, D. Jia, M. Yang, N. Zhang, Q. Qu, Z. Han, K. Sun, Heat transfer performance of MQL grinding with different nanofluids for Ni-based alloys using vegetable oil, J. Clean. Prod. 154 (2017) 1–11.
[34] S. Guo, C. Li, Y. Zhang, Y. Wang, B. Li, M. Yang, X. Zhang, G. Liu, Experimental evaluation of the lubrication performance of mixtures of castor oil with other vegetable oils in MQL grinding of nickel-based alloy, J. Clean. Prod. 140 (2017) 1060–1076.
[35] Y. Wang, C. Li, Y. Zhang, B. Li, M. Yang, X. Zhang, S. Guo, G. Liu, Experimental evaluation of the lubrication properties of the wheel/workpiece interface in MQL grinding with different nanofluids, Tribol. Int. 99 (2016) 198–210.
[36] T. Gao, C. Li, D. Jia, Y. Zhang, M. Yang, X. Wang, H. Cao, R. Li, H.M. Ali, X. Xu, Surface morphology assessment of CFRP transverse grinding using CNT nanofluid minimum quantity lubrication, J. Clean. Prod. 277 (2020), 123328.
[37] M. Yang, C. Li, Y. Zhang, D. Jia, R. Li, Y. Hou, H. Cao, J. Wang, Predictive model for minimum chip thickness and size effect in single diamond grain grinding of zirconia ceramics under different lubricating conditions, Ceram. Int. 45 (12) (2019) 14908–14920.
[38] T. B, C.H. Huang, Y.B. Li, W.F. Zhang, M. Ding, Y.Y. Yang, H. Yang, X.F. Zhai, D.Z. Xu, S. Wang, M. Debnath, H.N. Jamil, H.M. Li, M.K. Ali, Gupta, Z. Said, Advances in fabrication of ceramic corundum abrasives based on sol–gel process, Chin. J. Aeronaut. 34 (6) (2021) 1–17.
[39] J. Zhang, C. Li, Y. Zhang, M. Yang, D. Jia, G. Liu, Y. Hou, R. Li, N. Zhang, Q. Wu, H. Cao, Experimental assessment of an environmentally friendly grinding process using nanofluid minimum quantity lubrication with cryogenic air, J. Clean. Prod. 193 (2018) 236–248.
[40] X. Wang, C. Li, Y. Zhang, Z. Said, S. Debnath, S. Sharma, M. Yang, T. Gao, Influence of texture shape and arrangement on nanofluid minimum quantity lubrication turning, The. Int. J. Adv. Manufact. Techn. 119 (1–2) (2022) 631–646.
[41] Y.Y. Yang, Y.D. Gong, C.H. Li, X.L. Wen, J.Y. Sun, Mechanical performance of 316L stainless steel by hybrid directed energy deposition and thermal milling process, J. Mater. Process. Technol. 291 (2021), 117023.
[42] W. Qiao, Z. Fu, M. Du, N. Wei, E. Liu, Seasonal peak load prediction of underground gas storage using a novel two-stage model combining improved complete ensemble empirical mode decomposition and long short-term memory with a sparrow search algorithm, Energy 274 (2023), 127376, https://doi.org/10.1016/j.energy.2023.127376.
[43] V. Alankaya, A. Sinan, Oktem Static analysis of laminated and sandwich composite doubly-curved shallow shells, Steel, Compos. Struct. 20 (5) (2016) 1043–1066.
[44] F. Tornabene, A. Ceruti, Free-form laminated doubly-curved shells and panels of revolution resting on winkler-pasternak elastic foundations. A 2-D gdq solution for static and free vibration analysis, World J. Mech. 3 (2013) 1–25.
[45] A. Veysi, R. Shabani, G. Rezazadeh, Nonlinear vibrations of micro-doubly curved shallow shells based on the modified couple stress theory, Nonlinear Dynam. 87 (2017) 2051–2065.
[46] S.N. Thakur, C. Ray, S. Chakraborty, A new efficient higher-order shear deformation theory for a doubly curved laminated composite shell, Acta Mech. 228 (1) (2017) 69–87.
[47] Y. Kiani, M. Shakeri, M.R. Eslami, Thermoelastic free vibration and dynamic behavior of an FGM doubly curved panel via the analytical hybrid Laplace–Fourier transformation, Acta Mech. 223 (2012) 1199–1218.
[48] M. Arefi, Analysis of a doubly curved piezoelectric nano shell. nonlocal electro-elastic bending solution, Eur. J. Mech. Solid. 70 (2018) 226–237.
[49] M. Arefi, R.K. Faegh, A. Loghman, The effect of axially variable thermal and mechanical loads on the 2D thermoelastic response of FG cylindrical shell, J. Therm. Stresses 39 (12) (2016) 1539–1559.
[50] M. Arefi, K.K. Żur, Free vibration analysis of functionally graded cylindrical nanoshells resting on Pasternak foundation based on two-dimensional analysis, Steel Compos. Struct. 34 (4) (2020) 615–623.
[51] L. Xie, Y. Zhu, M. Yin, Z. Wang, D. Ou, H. Zheng, G. Yin, Self-feature-based point cloud registration method with a novel convolutional Siamese point net for optical measurement of blade profile, Mech. Syst. Signal Process. 178 (2022), 109243, https://doi.org/10.1016/j.ymssp.2022.109243.
[52] Z. Wang, C. Chen, H. Liu, D. Hrynshpan, T. Savitskaya, J. Chen, J. Chen, Enhanced denitrification performance of Alcaligenes sp. TB by Pd stimulating to produce membrane adaptation mechanism coupled with nanoscale zero-valent iron, Sci. The. Total. Env. 708 (2020), 135063, https://doi.org/10.1016/j.scitotenv.2019.135063.
[53] Q. Fu, M. Gu, J. Yuan, Y. Lin, Experimental study on vibration velocity of piled raft supported embankment and foundation for ballastless high speed railway, Buildings 12 (11) (2022) 1982, https://doi.org/10.3390/buildings12111982.
[54] C. Liu, J. Cui, Z. Zhang, H. Liu, X. Huang, C. Zhang, The role of TBM asymmetric tail-grouting on surface settlement in coarse-grained soils of urban area. Field tests and FEA modelling, Tunn. Undergr. Space Technol. 111 (2021), 103857, https://doi.org/10.1016/j.tust.2021.103857.
[55] S. Yang, X. Li, T. Yu, J. Wang, H. Fang, F. Nie, L. Zheng, High-Performance neuromorphic computing based on ferroelectric synapses with excellent conductance linearity and symmetry, Adv. Funct. Mater. 32 (35) (2022), 2202366, https://doi.org/10.1002/adfm.202202366.
[56] C. Zhong, H. Li, Y. Zhou, Y. Lv, J. Chen, Y. Li, Virtual synchronous generator of PV generation without energy storage for frequency support in autonomous microgrid, Int. J. Electr. Power Energy Syst. 134 (2022), 107343, https://doi.org/10.1016/j.ijepes.2021.107343.
[57] X. Zhang, Y. Wang, M. Yang, G. Geng, Toward concurrent video multicast orchestration for caching-assisted mobile networks, IEEE Trans. Veh. Technol. 70 (12) (2021) 13205–13220, https://doi.org/10.1109/TVT.2021.3119429.